9-1-2016

Microdose Fluorescence Imaging of ABY-029 on an Operating Microscope Adapted by Custom Illumination and Imaging Modules

Jonathan T. Elliott
Dartmouth College

Alisha V. Dsouza
Dartmouth College

Kayla Marra
Dartmouth College

Brian W. Pogue
Dartmouth College

David Roberts
Dartmouth College

See next page for additional authors

Authors
Jonathan T. Elliott, Alisha V. Dsouza, Kayla Marra, Brian W. Pogue, David Roberts, and Keith Paulsen

Research Article | Vol. 7, No. 9 | 1 Sep 2016 | BIOMEDICAL OPTICS EXPRESS 3280
Biomedical Optics EXPRESS

Microdose fluorescence imaging of ABY-029 on an operating microscope adapted by custom illumination and imaging modules

JONATHAN T. ELLIOTT,[1] ALISHA V. DSOUZA,[1] KAYLA MARRA,[1] BRIAN W. POGUE,[1,2] DAVID W. ROBERTS,[2,3] AND KEITH D. PAULSEN[1,2]

[1]*Center for Imaging Medicine, Thayer School of Engineering, Dartmouth College, 1 Medical Center Drive, Lebanon, NH 03756, USA*
[2]*Department of Surgery, Geisel School of Medicine at Dartmouth, 1 Rope Ferry Road, Hanover, NH 03755, USA*
[3]*Neurosurgery Section, Dartmouth-Hitchcock Medical Center, 1 Medical Center Drive, Lebanon, NH 03756, USA*
** Jonathan.T.Elliott@dartmouth.edu*

Abstract: Fluorescence guided surgery has the potential to positively impact surgical oncology; current operating microscopes and stand-alone imaging systems are too insensitive or too cumbersome to maximally take advantage of new tumor-specific agents developed through the microdose pathway. To this end, a custom-built illumination and imaging module enabling picomolar-sensitive near-infrared fluorescence imaging on a commercial operating microscope is described. The limits of detection and system specifications are characterized, and *in vivo* efficacy of the system in detecting ABY-029 is evaluated in a rat orthotopic glioma model following microdose injections, showing the suitability of the device for microdose phase 0 clinical trials.

OCIS codes: (170.1610) Clinical applications; (170.3880) Medical and biological imaging; (170.4730) Optical pathology; (260.2510) Fluorescence.

References and links

1. A. L. Vahrmeijer, M. Hutteman, J. R. van der Vorst, C. J. van de Velde, and J. V. Frangioni, "Image-guided cancer surgery using near-infrared fluorescence," Nat. Rev. Clin. Oncol. **10**(9), 507–518 (2013).
2. Q. T. Nguyen and R. Y. Tsien, "Fluorescence-guided surgery with live molecular navigation--a new cutting edge," Nat. Rev. Cancer **13**(9), 653–662 (2013).
3. B. E. Schaafsma, J. S. Mieog, M. Hutteman, J. R. van der Vorst, P. J. Kuppen, C. W. Löwik, J. V. Frangioni, C. J. van de Velde, and A. L. Vahrmeijer, "The clinical use of indocyanine green as a near-infrared fluorescent contrast agent for image-guided oncologic surgery," J. Surg. Oncol. **104**(3), 323–332 (2011).
4. G. M. van Dam, G. Themelis, L. M. Crane, N. J. Harlaar, R. G. Pleijhuis, W. Kelder, A. Sarantopoulos, J. S. de Jong, H. J. Arts, A. G. van der Zee, J. Bart, P. S. Low, and V. Ntziachristos, "Intraoperative tumor-specific fluorescence imaging in ovarian cancer by folate receptor-α targeting: first in-human results," Nat. Med. **17**(10), 1315–1319 (2011).
5. W. Stummer, U. Pichlmeier, T. Meinel, O. D. Wiestler, F. Zanella, and H. J. Reulen, "Fluorescence-guided surgery with 5-aminolevulinic acid for resection of malignant glioma: a randomised controlled multicentre phase III trial," Lancet Oncol. **7**(5), 392–401 (2006).
6. E. L. Rosenthal, B. D. Kulbersh, T. King, T. R. Chaudhuri, and K. R. Zinn, "Use of fluorescent labeled anti-epidermal growth factor receptor antibody to image head and neck squamous cell carcinoma xenografts," Mol. Cancer Ther. **6**(4), 1230–1238 (2007).
7. A. V. Dsouza, H. Lin, E. R. Henderson, K. S. Samkoe, and B. W. Pogue, "Review of fluorescence guided surgery sytems: identification of key performance capabilities beyond indocyanine green imaging," J. Biomed. Opt. (2016, Accepted July 19).
8. J. T. Elliott, K. Marra, L. T. Evans, S. C. Davis, K. S. Samkoe, J. D. Olson, J. Feldwisch, K. D. Paulsen, D. W. Roberts, and B. W. Pogue, "Simultaneous in vivo fluorescent markers for perfusion, protoporphyrin metabolism and EGFR expression for optically guided identification of orthotopic glioma," Clin. Cancer Res. under review.
9. Food and Drug Administration, "Guidance for Industry, Investigators, and Reviewers: Exploratory IND Studies," Office of Training and Communication **HFD-240** (2006).

#267813 http://dx.doi.org/10.1364/BOE.7.003280
Journal © 2016 Received 6 Jun 2016; revised 14 Jul 2016; accepted 3 Aug 2016; published 9 Aug 2016

Biomedical Optics EXPRESS

10. J. T. Elliott, A. V. Dsouza, S. C. Davis, J. D. Olson, K. D. Paulsen, D. W. Roberts, and B. W. Pogue, "Review of fluorescence guided surgery visualization and overlay techniques," Biomed. Opt. Express **6**(10), 3765–3782 (2015).
11. T. Kuroiwa, Y. Kajimoto, and T. Ohta, "Development of a fluorescein operative microscope for use during malignant glioma surgery: a technical note and preliminary report," Surg. Neurol. **50**(1), 41–49 (1998).
12. P. A. Valdés, F. Leblond, V. L. Jacobs, B. C. Wilson, K. D. Paulsen, and D. W. Roberts, "Quantitative, spectrally-resolved intraoperative fluorescence imaging," Sci. Rep. **2**, 798 (2012).
13. J. R. Watson, C. F. Gainer, N. Martirosyan, J. Skoch, G. M. Lemole, Jr., R. Anton, and M. Romanowski, "Augmented microscopy: real-time overlay of bright-field and near-infrared fluorescence images," J. Biomed. Opt. **20**(10), 106002 (2015).
14. D. B. Hoelzinger, L. Mariani, J. Weis, T. Woyke, T. J. Berens, W. S. McDonough, A. Sloan, S. W. Coons, and M. E. Berens, "Gene expression profile of glioblastoma multiforme invasive phenotype points to new therapeutic targets," Neoplasia **7**(1), 7–16 (2005).

1. Introduction

Fluorescence guided surgery (FGS) is emerging as an important tool for bulk tumor resection, with the potential to positively impact several different areas of surgical oncology [1–6]. One of the challenges to evaluating the potential of FGS—more specifically, the efficacy of various imaging agent/device pairs—is that the engineering demands of each subspecialty of surgical oncology are different. Because the field is in relative infancy, and in order to reach the largest potential customer base as possible, companies have developed general-use signal fluorescence imaging systems. These were reviewed in a recent paper [7], and showed marked variability in performance, features, and clinical ease-of-use. In recent years, neurosurgery has led the way in terms of bringing fluorescence guided surgery to fruition—it is no coincidence that neurosurgery is usually performed with an operating microscope over a relatively small, relatively flat, and often uniform field of view. These three features—with the first being arguably the most important—have made the addition of light sources and filter sets to the standard microscope hardware relatively straight-forward. The integrity of the blood-brain barrier except where compromised by the tumor has enabled the off-label use of already approved but large, non-specific dyes at large doses due to their pre-existing safety record, resulting in protocols that are easy to implement and robust even when deployed in a qualitative manner. Because many tumors are not adequately enhanced by these large molecules, a new wave of imaging agents are being developed that are tumor-specific and more efficacious in identifying tumor margins and low-grade gliomas.

The abilities of current fluorescence-capable operating microscopes, such as the Zeiss Pentero and Leica M530 OH6, are being pushed to their limit by a desire to image eIND agents approved under the microdose pathway [8]—an infrared epidermal growth factor receptor targeted small molecule imaging agent which has shown promise in orthotopic rat gliomas after *in vivo* administration—this paper presents an in-house modified version of the Zeiss Pentero for the purpose of detecting microdose levels of ABY-029 during glioma resection. Because ABY-029, as well as other in-development agents, rely on the microdose pathway of FDA approval (where levels of agent are administered to humans at doses between 30 nanomoles and 100x lower than those known to cause any physiological effects), the levels of fluorescence remitted by the tissue are often lower than the noise floor of current commercial systems.

This paper demonstrates a practical, straight-forward approach to greatly enhancing the capabilities of current surgical imaging systems, remaining within safety limits for emission and skin exposure, and without compromising the workflow of the surgeon. The engineering criteria for this adapted set-up emerged from a previous review paper, and include: high sensitivity (< 10 nM) to tracer of interest, real-time overlay of white-light and fluorescence images; fluorescence mode operation with ambient room lighting present; ability to quantify tracers *in situ*; ability to image multiple fluorophores simultaneously; and maximized ergonomic use. These were identified as the leading criteria for the current clinical and preclinical R&D climate, and as such, we evaluate our adapter solution in light of these criteria.

Biomedical Optics EXPRESS

2. Materials and methods

Instrumentation

The system consists of a detection module and an illumination module (Fig. 1). The detection module is attached to the microscope via a custom machined Zeiss accessory port adapter, which contains a 5-mm diameter VIS-NIR coated achromatic doublet lens (effective focal length = 125 mm; Stock #49-361, Edmund Optics, Barrington, NJ). The distal end of the adapter is joined to a dichroic mirror cage (C4W, Thorlabs, Newton, NJ) containing a dichroic filter element which reflects light less than 770-nm and transmits light above 770-nm (T770lpxr, Chroma, Bellows Falls, VT). A c-mount adapter enables attachment of the RGB camera (acA1920-155uc, Basler, Ahrensburg, Germany) to a rotational element (CRM1L, Thorlabs) to facilitate alignment with the fluorescence channel. This element is attached to the reflection window of the dichroic cage. Attached to the transmission window is a threaded cage plate (SP6S, Thorlabs) holding a long-pass filter (ET780lp, Chroma) to further exclude any excitation light that may have leaked through the dichroic. Affixed to the distal end of the holder is a c-mount adapter ring which enables attachment of the sCMOS camera (edge 4.1, PCO, Germany).

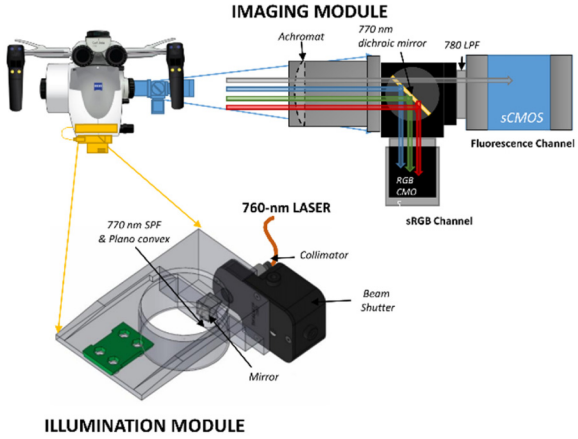

Fig. 1. The detection module (blue) and the illumination model (yellow) are attached to the Zeiss Pentero OPMI head and can be used without affecting standard operation of the microscope.

The infrared and RGB cameras are connected to PC via a custom camera link interface and a USB 3.0 interface, respectively, and are controlled by LABVIEW software and/or commercial software and libraries provided by the manufacturers. The illumination module consists of a 3D printed thermoplastic polymer adapter which houses a laser collimator (F220SMA-780, Thorlabs), a mechanical beam shutter (SH05, Thorlabs) a right-angle prism dielectric mirror (MRA12-E02, Thorlabs), a shortpass filter (ET770spuv, Chroma Technology Corp., Bellows Falls, VT) and a plano-concave lens (f = –25 mm; AD11FLC1054-B, Thorlabs).

The excitation light is generated with a 1.0 W continuous-wave 760-nm multi-transverse mode laser diode unit (DL760-1W, CrystaLaser LC, Reno, NV) and delivered via a 1-m multi-mode 200-μm core diameter 0.22-NA fiber (M25L01, Thorlabs) to the laser collimator SMA terminal on the adapter. From there the light passes through the beam shutter and is incident to the normal plane of the right-angle prism at a 47.375°, so that the reflected beam passes through the low-pass filter and plano-concave lens exiting the adapter at an angle of 4.75° relative to the vertical axis. This angle was chosen because it results in an illumination field centered on the optical axis of the microscope when the working distance is 300 mm, a

Biomedical Optics EXPRESS

typical operating parameter. The beam expansion and divergence caused by the plano lens results in a Gaussian-blurred top-hat profile which has a uniform diameter of approximately 65 mm and then rolls off gradually, resulting in a full width half maximum (FWHM) of about 80 mm for the entire illumination field. The entire unit produces Class 3R emission as evaluated by IEC 60825-1 standards (< 185 mW measured 70 mm from light exit by a 7 mm diameter power meter sensor (PM100D, Thorlabs) and is appropriately labeled according to these standards. The illumination as a function of microscope focal length is provided in Fig. 2(b), with typical distances used during open craniotomy between 180 and 350 mm.

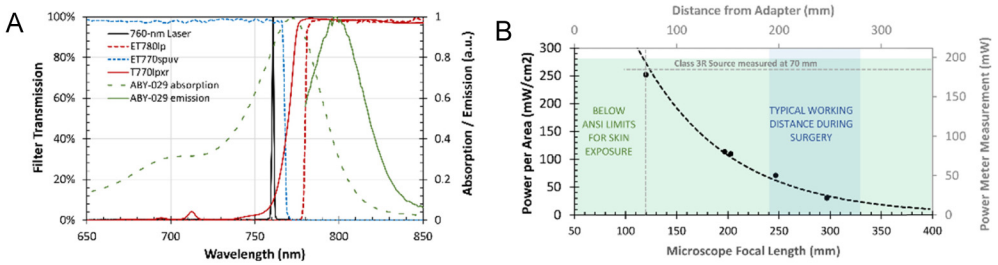

Fig. 2. (A) The laser (black line) is cleaned up by the ET770spuv shortpass filter before exiting the illumination module. This excitation along with coincident white-light from the Pentero is reflected by the T770lpxr dichroic towards the RGB camera. The fluorescence emission is transmitted through the dichroic and filtered by the ET780lp long-pass filter before sCMOS detection. (B) Maximum laser beam power, measured in the center of the illumination field was characterized using a power meter affixed with a 7-mm diameter aperture at different distances from the bottom of the adapter. The green shaded area indicates power per area below the ANSI limit for skin exposure for a continuous-wave 760 nm light source. The blue shaded area shows the typical working distance used during surgery. The IEC 3R Laser class limit is represented by the dashed grey line.

Figure 2(a) shows the filter transmissions of the modules, based on values provided from manufacturers, and the ABY-029 absorption and emission spectra measured by spectroscopy. Because of the relatively small Stokes shift compared with PpIX, an increased demand is placed on filter and light-source selection to maximize the sensitivity of the system. Instead of a more commonly available 730-nm laser, to enhance ABY-029 excitation a 1-W 760-nm laser was used. A dichroic mirror is used in combination with a long-pass filter to allow only light above 780 nm to enter the fluorescence-channel camera sensor, with an OD of 10-12 for wavelengths less than 765 nm (slightly lower if the incident angle is larger than 10 degrees, but under typical operating conditions where the region-of-interest is centered in the field-of-view, this is not as much of a concern). Light of shorter wavelengths than 770 nm is reflected to the RGB camera for white-light imaging. The specificity of the fluorescence channel to only infrared light arising from fluorophore emission enables integration of almost all the emission spectrum of ABY-029, to the extent which is permitted by the sCMOS sensor quantum efficiency which like all such sensors, degrades rapidly from 800 to 1000 nm. Because of a weak (OD 2.5) hot mirror built into the Zeiss white-light source—a filtered arc lamp—fluorescence imaging can be performed simultaneously while the arc lamp is on, if background subtraction is performed to reduce any contribution from infrared light that is not reflected internally. However, the arc lamp may weakly excite the fluorophore at wavelengths below 700 nm and therefore it is recommended that it be turned off for quantitation.

To protect the surgeon from accidental laser exposure due to specular reflection, which could be intensified by the magnifying optics of the microscope, short-pass filters with a cut-on at 725 nm (86-103, Edmund Optics, Barrington, NJ) were placed in the optical path of each eyepiece at the proximal side of the beam splitter module. This was done by mounting custom 18 mm diameter filters in a threaded metal ring, which is compatible with the internal threading of the Zeiss module (0.7500” x 32), constructed out of aluminum. The resulting ~6OD attenuation of the laser beam provides a Laser safety equivalent to Class 1, and since

Biomedical Optics EXPRESS

the Zeiss arc lamp is already fitted with a short-pass filter cutting on at 700 nm, no alterations in the surgeon's visual inspection of the field occur.

Animal experiments

All experiments were conducted according to a protocol approved by the Dartmouth Institutional Animal Care and Use Committee (IACUC). Twelve rats (*Rattus norvegicus* Fischer 344 strain) were obtained from Charles River Laboratories (Wilmington, MA) and assigned to one of three groups: 1x (24.5 μg/kg), 3x (73.5 μg/kg) and 6x (147 μg/kg) microdose. Each rat was anesthetized with 1-3% isofluorane, and 1 x 106 F98 EGFR-positive cells (ATCC CRL-2948) cultured at 37°C in DMEM with 10% (v/v) FBS and 1% penicillin-streptomycin were implanted stereotactically into the cortex 3-mm anterior to the bregma and about 4-mm lateral to the midline. Animals were monitored until they showed signs of weight-loss, an average of 23 days post-implantation. Intravenous injections of ABY-029 were given 2 hours prior to imaging at the assigned microdose level (1x, 3x, or 6x the rat equivalent microdose of 24.5 μg/kg according to FDA guidance [9]) along with 75 mg/kg of 5-aminoleuvulinic acid (A3785-500MG, Sigma Aldrich Co. LLC, St. Louis, MO). During imaging, animals were anesthetized (isofluorane 3-4%) and the scalp was dissected and removed using a scalpel. Craniotomy was performed using a rotary drill tool (Model 8220, Dremel, Racine, WI), carefully thinning the skull in a ~10 mm diameter circumferential path until it could be lifted off of the dura surface. Once hemostasis was achieved, the animal was imaged on each system for ABY-029 and PpIX. The animal was euthanized and the brain was removed intact, with imaging performed in the same manner as well as on the LI-COR Pearl.

3. Results and discussion

System characterization

Under typical operating conditions of 300-mm focal length and 2.0x zoom, the resolution of the RGB channel is 70 μm (USAF 1951 Test Target 3(6), 14.25 lp/mm) and the resolution of the infrared channel is 250 μm (USAF 1951 Test Target 2(1), 4.00 lp/mm). In comparison, the Zeiss Pentero has a resolution of 56 μm (USAF 1951 Test Target 4(2), 17.96 lp/mm) when directly observing the white-light reflectance in the microscope occulars and when measured on the white-light images captured by the internal camera, and 281 μm (USAF 1951 Test Target 1(6), 3.56 lp/mm) for tungsten-light illuminated target captured by the camera in IR800 mode. Field of view measured at 1x zoom was 112 mm x 70 mm for the RGB camera and 164 mm x 140 mm for the fluorescence camera, compared with 132 mm x 104 mm for the Zeiss built-in camera. The depth of field (DOF) or effective focus range of the fluorescence and RGB channels were compared with the Pentero built-in camera and the observations made directly using the Pentero oculars using a DOF 5-15 target (54-440, Edmund Optics). Following the correct placement of the target at the 300-mm focal length, depth of field was determined for 5 lp/mm to be 20 mm for the RGB and fluorescence channels, respectively, and 15 mm for the Zeiss built-in camera. Direct observation through the oculars enabled greater than 5 lp/mm resolution across a DOF of 40 mm. The color acquisition properties of the RGB camera were also evaluated using the standard Macbeth colorchecker card, and calibrated accordingly. Following calibration, the median difference between colors acquired on the Basler RGB camera and the Zeiss built in camera were 2%, 2%, and 4% of the color dimension for red, green and blue channels, respectively, with maximum discrepancies being 10%, 11%, and 13% for those same channels, respectively. The percent difference between the whitepoints was 5%.

Phantom experiments

The sensitivity of the microdose-adapted Pentero system measured in phantoms with low ambient light only, and with the arc lamp on at 30% power, were compared with the built-in

Biomedical Optics EXPRESS

IR800 channel and the LI-COR Impulse Pearl to determine the range of detectible ABY-029 concentrations for each configuration (Fig. 3).

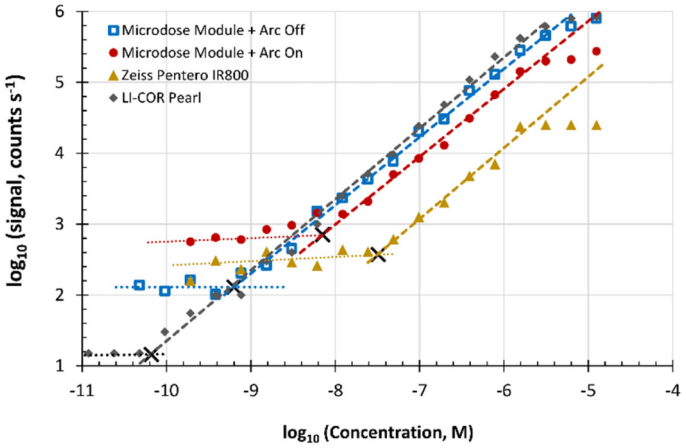

Fig. 3. The relationship between signal and ABY-029 concentration for each system plotted on a log-log scale. When evaluating the microdose module, the Pentero xenon arc lamp was either off (squares) or on at 30% power (dots). Dashed lines show the line-of-best-fit over the linear response regions, and dotted lines show the noise floor. Black crosses show the intersection point which defines the lower limit of detection.

Exposure times of 50 ms, 100 ms, 200 ms, 500 ms, and 1000 ms were acquired with a rolling shutter, using 4x4 pixel binning, at a working distance of 250 mm and light intensity of 30 mW/cm^2. The noise floor level was quantified by fitting the signal obtained with the undetectable sample tubes, and the linear portion of the sensitivity curve was fit with a line-of-best-fit to determine the signal response of the system to linearly increasing concentrations of dye. The lower limit of detection was defined as the point of intersection of the noise floor slope and the linear region line-of-best-fit. The Pearl had the lowest limit of detection, 66 pM, followed by the adapted Pentero under low ambient light conditions, which could detect as low as 630 pM concentrations. With the arc light operating at 30%, the sensitivity was reduced to 7 nM. The IR800 channel had the poorest lower limit of detection, with 32 nM. All configurations showed highly linear responses within the range of detectable concentrations, having slopes between 0.96 and 1.05.

Dynamic range (calculated as the difference between log2 maximum signal and noise floor) varied widely across systems. The highest effective dynamic range, defined as the range of intensities in the linear region for ABY-029 detection, was provided by the LI-COR Pearl (16-bit) and the microdose-adapted Pentero (12-bit). Performance of the microdose-adapted Pentero was limited slightly by simultaneous operation of the Xenon arc lamp increasing the background signal, but still provided 8-bit dynamic range. The Zeiss Pentero IR 800 had the least usable dynamic range (6-bit), since it uses an 8-bit internal camera to capture the signal and had the second-highest noise floor.

Orthotopic glioma experiments

Figure 4 shows a selection of representative images acquired with the Pentero custom adapted system, the Pentero IR800 channel and the Pentero BLUE400 channel during craniotomy in vivo and after removal of the brain ex vivo. The Impulse Pearl was also used to image the sample ex vivo, representing an upper bounds on the performance limits of a clinical planar fluorescence imaging system. While the Pentero provided reliable images of PpIX emission, it was unable to image the ABY-029 emission from any of the dose levels, despite ROI analysis showing some difference in signal between tumor and background regions. The custom system was capable of providing highly detailed images of both white-light RGB and

Biomedical Optics EXPRESS

fluorescence from ABY-029 and PpIX. Of particular note, fluorescence emission at the 3x and 6x levels could be reliably detected and visualized as either a parametric map or as an overlay with the RGB image below, where the fluorescence intensity is visualized by solid green with transparency being determined by a logistic function ($L = 0.5$, $x_0 = 0.4$, $k = 0.2$) which is described in a previous review paper [10]. For 3x and 6x dose levels, the Zeiss Pentero Xenon arc lamp could be operated simultaneously with fluorescence imaging, provided that a background fluorescence image was acquired first. This represents a significant improvement over the cumbersome functionality of the Pentero which requires switching between normal white-light mode and IR800 mode.

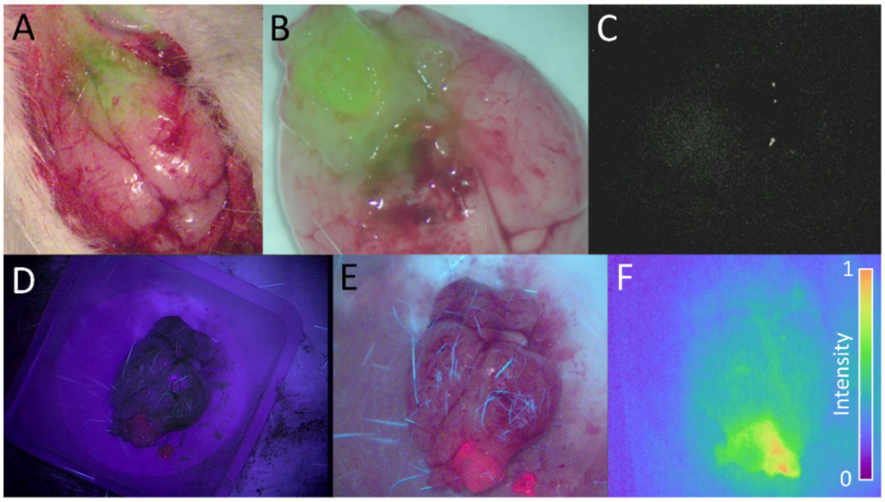

Fig. 4. (A) The overlay (fusion) of two images acquired simultaneously during open craniotomy with the custom imaging module: the RGB white-light image and the fluorescence image overlay 2-h following a 3x microdose injection. (B) The ex vivo overlay of the whole brain acquired 2-h following a 6x microdose injection. (C) The corresponding ex vivo fluorescence image acquired with the Pentero IR800 channel. (D) A PpIX image acquired with the Zeiss Pentero BLUE400 channel, and (E) the same brain imaged by the custom imaging module during blue-light excitation. (F) The same brain as in D and E, imaged for ABY-029 fluorescence using the customized Pentero 2-h following a 3x microdose injection.

The figures of merit used to evaluate the clinical efficacy of this device are the tumor-to-background ratio (TBR) and signal-to-noise ratio (SNR). Table 1 shows mean TBR and SNR values of each imaging system at each dose level. The LI-COR Impulse Pearl showed the highest contrast levels at all microdoses and the highest SNR; this device represents the state-of-the-art planar fluorescence imaging system at ideal acquisition conditions (*e.g.*, cooling, multilevel exposure, completely dark enclosure). The Pentero fitted with the microdose illumination and detection modules exhibited consistently high contrast in the 6x dose levels and moderate but detectable levels of tumor to background contrast in the 3x and 1x dose levels; SNR was high in all three levels. For this particular tumor line, which is a low-moderate expresser of EGFR, the enhancement by the lower two doses is very close to the limits of detection for this adapted system. The Pentero's built-in IR800 channel showed faint contrast at the 6x level, but when windowed and leveled, was noisy and contained no usable spatial information. The 95% confidence intervals show the high variability in IR800 measurements compared with the other two configurations, and the 1x and 3x dose levels exhibited SNRs of equal or less than 5, failing the Rose criterion.

Biomedical Optics EXPRESS

Table 1. The tumor to background ratio (TBR) and signal to noise ratio (SNR) determined for each dose level using each system. Values are group means with the 95% confidence interval of TBR indicated in parenthesis.

Dose (µg/kg)	*Zeiss Pentero microdose module*		*Zeiss Pentero IR800 mode*		*LI-COR Impulse Pearl*	
	TBR	*SNR*	*TBR*	*SNR*	*TBR*	*SNR*
24.50	1.4 (1.1 - 1.6)	12	1.1 (–0.2 - 2.5)	2	1.8 (1.2 - 2.3)	43
73.50	1.5 (1.2 - 1.8)	27	1.1 (–1.7 - 3.9)	5	3.2 (2.5 - 4.0)	105
147.0	3.2 (2.1 - 4.2)	60	1.5 (–2.4 - 5.8)	23	4.8 (3.4 - 6.3)	311

Clinical relevance

Presently, both Zeiss and Leica offer systems that can visualize fluorescence from protoporphyrin IX, fluorescein sodium and indocyanine green. These are administered in doses of 2 to 20 mg/kg depending on the dye being used, compared with the 3.4 µg/kg microdose given to a 70 kg adult. Therefore, these systems are optimized to detect 1,000-10,000x higher levels of fluorophore than would be expected from microdose-level injections, if all else is equal. This is evinced by the low TBR and SNR shown by the Zeiss IR800 at any of the three doses, and in particular, the high variability in these images. Commercial systems produced by at least seven different companies have claimed to detect nanomolar levels of concentration in vivo [7]; FDA-approved systems include Fluoptics Fluobeam, Quest Spectrum, Visionsense, Novadaq SPY and PDE Neo, and all are stand-alone systems that would be used in addition to the surgical microscope which is the most common platform for neurosurgical oncology. The main goal of this work is to provide a clinical platform for which experimental imaging agents can be developed and tested with minimal disruption to the workflow. The result was the development of a system which surpasses current clinical systems in the ability to detect and visualize IR fluorescence, yet is more easily integrated into the operating room setting than stand-alone investigational systems since it attaches to the Zeiss Pentero OPMI without affecting its clinical use, and provides real-time merged video of white-light RGB and color-map representation of 16-bit fluorescence. Furthermore, the light source is a Class 3R device emitting a large, divergent, monochromatic beam and can be safely used without additional personal protective equipment or concern of patient overexposure, yet provides high power (~30 mW/cm2) at typical working distances and supports simultaneous use with the Pentero Xenon arc lamp. Real-time acquisition of white-light RGB video enables fluorescent overlays to be updated continuously on a secondary monitor [10].

Custom systems that adapt a surgical microscope to fluorescence imaging have reported as early as 1998 [11]. More recently, our group demonstrated hyperspectral imaging of PpIX using a liquid crystal tunable filter enabled system using a similar adapter coupling, but without a custom illumination solution [12]. Other near infrared adaptations to operating microscopes have been reported [13], however, they have similar sensitivity than that provided by the IR800 channel and are therefore not suitable for microdose clinical trials. This work demonstrates a picomolar-sensitive device that serves a generalizable platform for future infrared eIND studies in surgeries indicating the use of an operating microscope. In a very recent study, the efficacy of ABY-029 was evaluated in fresh tissue sections of F98 wild-type and EGFR positive glioma-bearing rat brains following a 2x-microdose injection [8]. ABY-029 outperformed PpIX in EGFR-positive tumors in efficacy, and the combination of ABY-029 and PpIX fluorescence was complimentary and provided additional discriminatory power compared with each alone. These data demonstrated the specificity of ABY-029 for EGFR at levels expected in typical human low-grade and high-grade gliomas. However, the fluorescence measurements were obtained using a flatbed tissue section scanner, which is very sensitive and not capable of in vivo measurements. In this paper, we demonstrate for the

Biomedical Optics EXPRESS

first time that ABY-029 microdose level fluorescence can be detected and visualized using a clinically compatible system in an orthotopic glioma expressing low- to moderate levels of human EGFR, similar to levels found in many human brain tumors. Taken together, this suggests that microdose levels of ABY-029 imaged with the modified operating microscope have the real possibility of highlighting even low-grade human gliomas, for which EGFR expression may precede metabolic changes required for PpIX enhancement [14]. Moving forward, we hope to use this platform in a Phase 0 observational study to evaluate the efficacy of ABY-029 microdose imaging in human subjects undergoing glioma resection. By evaluating the contrast of ABY-029 in the bulk tumor, and more importantly, in the infiltrating margins, it is hoped that ABY-029 will show the same degree of efficacy it has shown in preclinical results to date and provide a benefit in resection guidance over current PpIX strategies.

4. Conclusion

This study highlights a powerful and easily deployable means to detect microdose-level infrared fluorescence during microscope-heavy surgical procedures such as open craniotomies. As proof-of-principle, the promising new imaging agent ABY-029 was imaged during live craniotomies in orthotopic tumor bearing rats, and was detectable at all microdose levels. Given the recently proposed microdose pipeline as a viable means to bring novel contrast agents to phase 0 clinical trials, we hope this or similar devices will find traction with clinical and academic researchers who wish to evaluate the next generation of tumor-specific dyes.

Funding

The authors would like to acknowledge funding support from the National Institutes of Health (R01CA109558 [BWP], R01CA167413 [BWP] and R01NS052274 [DWR]) as well as a CompX Faculty Grant from the William H. Neukom 1964 Institute for Computational Science (JTE).

Acknowledgments

We would like to thank the members of the Dartmouth-Hitchcock Neurosurgery Research Team, in particular Dr. Linton Evans and Jonathan Olson, as well as Prof. Scott C. Davis and Dr. Vincent Rossi for helpful discussions.